

A SIMPLE MODEL FOR CALCULATING THE INDEX
OF REFRACTION OF NEON I AND NEON*(3s) IN
THE CAVITY OF A XENON FLUORIDE LASER

James Etchechury

NAVAL POSTGRADUATE SCHOOL

Monterey, California



THESIS

A SIMPLE MODEL FOR CALCULATING THE INDEX
OF REFRACTION OF NEON I AND NEON*(3s) IN
THE CAVITY OF A XENON FLUORIDE LASER

by

James Etchechury
June 1979

Thesis Advisor:

Allen E. Fuhs

Approved for public release; distribution unlimited.

Prepared for: Dr. Joseph Mangano
Defense Advanced Research Projects Agency
1400 Wilson Boulevard
Arlington, VA 22209

T 102316

UNCLASSIFIED

SECURITY CLASSIFICATION OF THIS PAGE (When Data Entered)

REPORT DOCUMENTATION PAGE		READ INSTRUCTIONS BEFORE COMPLETING FORM
1. REPORT NUMBER NPS 69-79-005	2. GOVT ACCESSION NO.	3. RECIPIENT'S CATALOG NUMBER
4. TITLE (and Subtitle) A SIMPLE MODEL FOR CALCULATING THE INDEX OF REFRACTION OF NEON I AND NEON*(3s) IN THE CAVITY OF A XENON FLUORIDE LASER.		5. TYPE OF REPORT & PERIOD COVERED Master's Thesis June 1979
7. AUTHOR(s) James Etchechury, Captain, U. S. Army		6. PERFORMING ORG. REPORT NUMBER
9. PERFORMING ORGANIZATION NAME AND ADDRESS Naval Postgraduate School Monterey, California 93940		8. CONTRACT OR GRANT NUMBER(s) ARPA Order Number 3747 (N0001479WR90174)
11. CONTROLLING OFFICE NAME AND ADDRESS Naval Postgraduate School Monterey, California 93940		10. PROGRAM ELEMENT, PROJECT, TASK AREA & WORK UNIT NUMBERS Proj Elem 62301E Program Code 9E20
14. MONITORING AGENCY NAME & ADDRESS (if different from Controlling Office) Dr. Robert Behringer ONR Branch Office 1030 East Green Street Pasadena, CA 91101 (213) 795-5971		12. REPORT DATE June 1979
		13. NUMBER OF PAGES 53
16. DISTRIBUTION STATEMENT (of this Report) Approved for public release; distribution unlimited		15. SECURITY CLASS. (of this report) UNCLASSIFIED
		15a. DECLASSIFICATION/DOWNGRADING SCHEDULE
17. DISTRIBUTION STATEMENT (of the abstract entered in Block 20, if different from Report)		
18. SUPPLEMENTARY NOTES		
19. KEY WORDS (Continue on reverse side if necessary and identify by block number) Beam Quality Metastable Neon Index of Refraction Excimer Laser Neon* Phase Velocity Neon Absorption Cross Section Phase Shift		
20. ABSTRACT (Continue on reverse side if necessary and identify by block number) A model for calculating the index of refraction of atomic species present in the cavity of a Xenon Fluoride Laser is applied to Neon and Neon*(3s). The model considers the variation from unity to be a function of the absorption cross section. Below the ionization threshold, the cross section is a set of discrete transitions between the various energy levels of the specie of concern. Above the 5p level, the discrete transitions become indistinct and the continuum cross section function is extended into this region.		

The continuum cross section function is a polynomial function fitted to independent research results. The results for Neon I agree with previous theoretical and experimental results. The model is extended to Neon*(3s). Comparison with the results of independent research of the polarizability and cavity phase shift derived from the calculation indicate accuracy is within ten percent.

A Simple Model for Calculating
the Index of Refraction of Neon I and Neon*(3s)
in the Cavity of a Xenon Fluoride Laser

James Etchechury
Captain, United States Army
B. S., United States Military Academy, 1970

Submitted in partial fulfillment of the
requirements for the degree of

MASTER OF SCIENCE IN PHYSICS

from the

NAVAL POSTGRADUATE SCHOOL
June 1979

ABSTRACT

A model for calculating the index of refraction of atomic species present in the cavity of a Xenon Fluoride laser is applied to Neon and Neon*(3s). The model considers the variation from unity to be a function of the absorption cross section. Below the ionization threshold, the cross section is a set of discrete transitions between the various energy levels of the specie of concern. Above the 5p level, the discrete transitions become indistinct and the continuum cross section function is extended into this region. The continuum cross section function is a polynomial function fitted to independent research results. The results for Neon I agree with previous theoretical and experimental results. The model is extended to Neon*(3s). Comparison with the results of independent research of the polarizability and cavity phase shift derived from the calculation indicate accuracy is within ten percent.

TABLE OF CONTENTS

ABSTRACT	4
LIST OF FIGURES.	6
TABLE OF SYMBOLS	7
I. INTRODUCTION	9
II. INDEX OF REFRACTION FROM DISPERSION THEORY . . .	16
III. THE OSCILLATOR STRENGTH	24
IV. THE ABSORPTION CROSS SECTION	27
V. CALCULATION OF THE INDEX OF REFRACTION OF NEON (2p6).	33
VI. CALCULATION OF THE INDEX OF REFRACTION OF NEON*(3s) ,	38
VII. COMPARISON OF RESULTS OF CALCULATION	
LIST OF REFERENCES	49
INITIAL DISTRIBUTION LIST.	53

LIST OF FIGURES

- Figure 1. XeF Laser Cavity Geometry
- Figure 2. Photoionization Cross Section of Neon ($2p^6$) in the Region 1.58 Ry to 3.3 Ry.
- Figure 3. Photoionization Cross Section of Neon ($2p^6$) in the Region 3.3 Ry to 11 Ry.
- Figure 4. Photoionization Cross Section of Neon* ($3s$) in the Region .365 Ry to 3.365 Ry.
- Figure 5. Energy Levels of Neon I and the Region of Discrete Oscillator Arrays and the Region of Extension of the Continuum Integral.
- Figure 6. Contribution of $3s \rightarrow 4p$ Transition to the Index of Refraction of Neon*($3s$).
- Figure 7. Sample Computer Output for the Calculation of the Contribution to the Index of Refraction of the $3s \rightarrow$ Transition. Laser Wavelength is 3510Å.
- Figure 8. Sample Computer Output for the Calculation of the Contribution to the Index of Refraction of the $3s \rightarrow 4p$ Transition. Laser wavelength is 3520Å.

LIST OF SYMBOLS

c	speed of light (3×10^{10} cm/sec)
C	constant defined in text
D	electric displacement vector
e	elementary charge (4.8031×10^{-10} esu)
E	electric field strength or energy of incident wave
f	oscillator strength of transition between two levels or configurations usually indicated as subscripts
g	degeneracy or quantum statistical weight of an energy level indicated as subscript
h, \hbar	Planck constant (4.1356×10^{-15} eV-s), ($\hbar = h/2\pi$)
i	$\sqrt{-1}$
i	index number
k	propagation vector
j, k	indices over lower (j) and upper (k) energy levels in a transition
K_e, K_m	relative permittivity, relative permeability
l	index over species in the cavity
ℓ	orbital quantum number
m, m_e	mass (gram), electron mass (9.11×10^{-28} g)
m, n	indices over lower (n) and upper (m) configurations of a transition array
\tilde{n}	complex index of refraction
n	real part of the complex index of refraction
n	principal quantum number
N	molecules (atoms)/cm ³
P	polarizability
R	constant defined in text

R	transition integral
A	angstrom (10^{-10} m)
γ	damping coefficient
ϵ, ϵ_0	permittivity
μ, μ_0	permeability
K	imaginary part of the complex index of refraction
ρ	density (g/cm^3)
σ	cross section
ϕ	spatial phase relation
ω	frequency (radians)
α	atomic polarizability

I. INTRODUCTION

The earliest successful high powered lasers operated in the vibration/rotation transitions of CO_2 and produced radiation in the infrared, principally in the 10.6 micron line. Extensive research and development of technology in the infrared laser field has produced impressive results that clearly demonstrate the feasibility of directed energy weapons utilizing these transitions for laser power production. The relatively long wavelength results in large optical components to form and direct the beam. Even though the highest power lasers are of the CO_2 type, their extremely large size limits their usefulness to laboratory experiments.

The shorter wavelength of chemical DF lasers provided improved efficiency and reduction in size of the power production and cavity components. This was the first laser system to demonstrate target engagement and destruction.¹ Still governed by the laws of diffraction, the optics were large and cumbersome.

Early work on the excimer lasers had demonstrated their ability to lase in the vacuum ultraviolet; however, problems with mirrors and competing absorption processes lead to low efficiencies for these lasers. The channeling of atomic

1. "International Defense Digest," International Defense Review, 12:316, Vol. 3, 1979.

ionization and excitation into these excited states was found to be very efficient. Further research by Velasco and Setzer produced interesting fluorescence in rare-gas halide combinations that led Ewing and Brau to the demonstration of the rare-gas halide exciplex laser, which is now included in the broad "excimer" description.²

The rare-gas monohalides are simple diatomic molecules which are bound in the excited state but are unstable or slightly bound in the ground state. The excited state of the excimer species can radiate in a broad band that is red shifted from the wavelength of the parent excitation. These lasers have demonstrated electrical efficiency as high as ten percent in various wavelengths, as depicted in Table I.

TABLE 1. Rare-gas Halide Laser Emission Wavelengths

	<u>Peak wavelengths of most intense band (nm)</u>			
	Ne	Ar	Kr	Xe
F	107 ^a	193	248	351,353
Cl	b	170	222	308
Br	b	166 ^{a,b}	206 ^a	282
I	b	b	185 ^{a,b}	252 ^a

(^aHas not demonstrated laser oscillation.)

(^bPredissociates, hence emission is weak or unobservable.)

2. Ewing, J. J., Rare-Gas Halide Lasers, Physics Today, May 1978, pp. 32-39.

Attempts to realize the inherent advantages of high electrical efficiency at short wavelength have resulted in extensive research and development activity in this area. Extensive literature on the kinematics of the excitation process and associated flow effects is available.^{3,4,5} There is a demonstrated understanding of the chemical kinetic processes involved in energy transfer and formation of the excited lasing molecules. Engineering development has demonstrated improved flow and acoustics effects. The latter were essential to the development of good beam quality in a demonstration device.⁶ In this case, good beam quality is considered to mean uniform phase across the cavity aperture. Nonuniform phase causes the peak axis intensity to fall off according to

$$\frac{I_{ff}}{I_o} = \exp [-(2\pi\phi_{rms}/\lambda)^2]$$

where ϕ_{rms} is obtained by squaring and averaging the phase shifts across the aperture. The spatial phase relation is

$$\phi = \int n ds.$$

3. Huestis, D. L., Small Scale Laser and Kinetics Program, paper presented at Rocketdyne International, Canoga Park, CA, 15 February 1979.

4. Hogge, H. D. and Crow, S. C., Flow and Acoustics in Pulsed Excimer Lasers, paper presented at AIAA Conference on Fluid Dynamics of High Power Lasers, II-4, Cambridge, MA, 2 November 1979.

5. Hogge, H. Dwight and Crow, Stephen, Flow Design Concepts for Pulsed Visible Wavelength Lasers, Darpa Report, May, 1978.

6. Siegler, R., et al., XeF Demonstrator Program, Rocketdyne International, 15 February 1979.

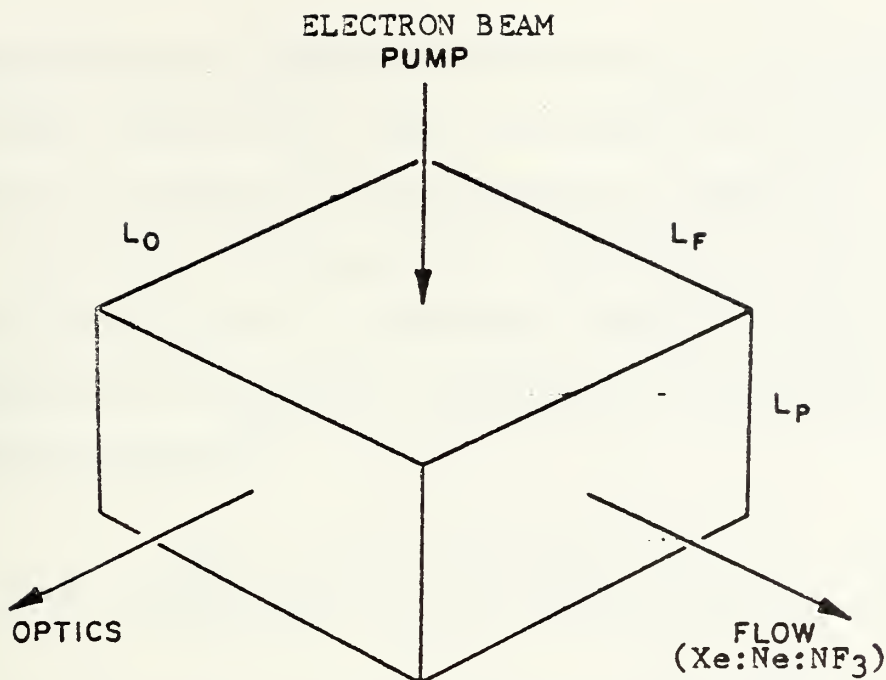


Figure 1. XeF Laser Cavity Geometry

The initial efforts to limit phase distortion considered the index of refraction in terms of the Gladstone-Dale formulation

$$n = 1 + G\rho$$

where G is the Gladstone-Dale constant, hence the concern for flow and acoustic effects. Hogge and Crow⁷ state that flow uniformity and reduced acoustic effects have achieved $\Delta\rho/\rho = 5 \times 10^{-5}$, the required flow uniformity.

It has been suggested, however, that the requirement for flow uniformity should be stated in terms of $\Delta n/n$ due to nonuniform pumping in the cavity.⁸ In a typical flow mixture,

7. Hogge, *ibid.*

8. Fuhs, A., Etchechury, J., and Cole, L., Progress Report #2, XeF Beam Quality Considerations, submitted to Dr. J. A. Mangano, DARPA, 25 February 1979.

the constituents of the medium (Ne:Xe:NF₃) are present in a fixed ratio (750:3:1).⁹ Even in a gas with fixed chemical composition, pressure and translational temperature, and hence, fixed $\Delta\rho/\rho$, $\Delta n/n$ can vary according to the ionic and electronic excitation of the medium caused by pumping.

Consider the Ladenburg formulation of the Kramers-Kronig dispersion relation¹⁰

$$n-1 = \frac{e^2 N}{2\pi m_e c^2} \sum_{\ell} \frac{N_{\ell}}{N} \sum_j \sum_k \frac{\lambda_{kj}^2 \lambda^2}{\lambda^2 - \lambda_{kj}^2} f_{kj} \left[1 - \frac{N_k g_j}{N_j g_k} \right] \quad \text{I-1}$$

There are ℓ distinct species indicating specific electronic or ionic excitation present in the cavity. Index j sums over lower levels and k over upper levels of possible configurations. Identify the mole fraction as

$$X_{\ell} = \frac{N_{\ell}}{N}, \quad \text{I-2}$$

the fraction of the total molecular population represented by species ℓ . Finally, define a quantity

$$T_{\ell} = \frac{e^2}{2\pi m_e c^2} \sum_j \sum_k \frac{\lambda_{kj}^2 \lambda^2}{\lambda^2 - \lambda_{kj}^2} f_{kj} \left[1 - \frac{N_k g_j}{N_j g_k} \right] \quad \text{I-3}$$

In terms of the quantities defined above

$$n - 1 = N \sum_{\ell} X_{\ell} T_{\ell} \quad \text{I-4}$$

9. Siegler, *ibid.*

10. Mitchell, A. C. G., and M. W. Zemansky, Resonance Radiation and Excited Atoms, p. 238, Cambridge, 1934.

or the index of refraction in the cavity is the sum of the contributions of all the species present in the cavity.

Since $N_\ell = NX_\ell$,

$$n - 1 = N_1T_1 + N_2T_2 + \dots \quad \text{I-5}$$

The partial density is given by $\rho_\ell = N_\ell m_\ell$, where m_ℓ is the molecular weight of ℓ th species. In terms of partial density, equation (I-5) becomes

$$n - 1 = \rho_1T_1/m_1 + \rho_2T_2/m_2 + \dots \quad \text{I-6}$$

Introduce the mass fraction for the gas mixture

$Y_\ell = \rho_\ell/\rho$, where ρ is the density of the gas mixture.

The result is

$$n - 1 = \rho[Y_1T_1/m_1 + Y_2T_2/m_2 + \dots] \quad \text{I-7}$$

Equation (I-7) shows that $n - 1$ is proportional to ρ ; however, equation (I-7) further demonstrates that $n - 1$ depends on mass fraction and index of refraction of each species. Even with uniform flow, the spatial phase relation across the cavity will not be uniform. Accurate modeling of the phase effects requires knowledge of the populations and the contribution to the index of refraction of the species in the cavity. This paper will explore a model for the index of refraction of the atomic species in the cavity and apply the model to neon.

In Section II, the formulation of the index of refraction to be applied in the current work will be derived. In Section III, the concept of transition arrays and the calculations of the transition array oscillator strengths

will be reviewed. The available data for the cross section of Neon I ($2p^6$) and Neon*(3s) will be reviewed in Section IV. The formulation derived in Section II will be applied to Neon I and the results compared to previous theoretical and experimental work in Section V. Section VI will discuss the calculations for Neon*(3s) and these results will be compared to independent experimental results in Section VII.

II. INDEX OF REFRACTION FROM DISPERSION THEORY

The ratio of the speed of light in a vacuum to the speed of light in a medium is known as the index of refraction,

$$n = \frac{c}{v} \quad \text{II-1}$$

where v is the phase velocity. Consider a simple wave

$$E = E_0 e^{i(\omega t - kx)} \quad \text{II-2}$$

where the phase relation is determined by

$$\omega t - kx = \text{constant} \quad \text{II-3}$$

Then

$$v = \frac{dx}{dt} = \frac{\omega}{k} . \quad \text{II-4}$$

Substitution of (4) into (1) yields

$$n = \frac{kc}{\omega} . \quad \text{II-5}$$

However, the index of refraction and propagation vector are frequency dependent, hence

$$n(\omega) = \frac{k(\omega)c}{\omega} . \quad \text{II-5A}$$

In terms of the relative permittivity and relative permeability of the medium

$$\sqrt{\frac{\epsilon}{\epsilon_0} \cdot \frac{\mu}{\mu_0}} = \sqrt{K_e \cdot K_m} \quad \text{II-6}$$

For gas lasers, as for most non-ferromagnetic elements, K_m does not vary significantly from unity.¹¹ This fact

yields Maxwell's Relation

$$n = \sqrt{K_e} = \sqrt{K_e(\omega)} \quad \text{II-7}$$

where K_e is the static dielectric constant of the medium at frequency ω .

The physical basis for the frequency dependence of n and the mechanism whereby the phase velocity in the medium varies slightly from c lies in the interaction of an incident electro-magnetic wave with the array of atoms constituting the dielectric material. In a gas, the molecules are sufficiently far apart that each molecule may be considered independent. The external field separates positive and negative charges which creates an additional field component known as the electric polarization (dipole moment per unit volume)

$$P = N\bar{x} \quad \text{II-8}$$

where N is the number of molecules per unit volume and \bar{x} is the average relative displacement of charge due to the external field. The following relations from Maxwell's equations hold

$$D = \epsilon E = \epsilon_0 K_e E = \epsilon_0 E + P \quad \text{II-9}$$

Simply stated, the electric displacement is proportional to the external field. We can write

$$K_e = 1 + \frac{P}{\epsilon_0 E} \quad \text{II-10}$$
$$\tilde{n} = \sqrt{K_e} = \sqrt{1 + \frac{P}{\epsilon_0 E}}$$

11. Hecht, E. and Zajac, A., Optics, Addison-Wesley Publishing Company, 1974.

where \tilde{n} is the complex index of refraction.

$$\tilde{n}^2 = 1 + \frac{P}{\epsilon_0 E} = 1 + \frac{N e \bar{x}}{\epsilon_0 E} . \quad \text{II-12}$$

For more than one dipole (as in array of N atoms)

$$\tilde{n} = 1 + \sum_N \frac{e \bar{x}}{\epsilon_0 E} \quad \text{II-13}$$

or the total change in the index of refraction is equal to the sum of the contributions of the dipoles.

An analytical expression for the average displacement of the charges is easily developed in classical terms of the Lorentz oscillator model of the atom. Although development of this model is properly done only with quantum mechanics, the classical treatment gives similar results. In the Lorentz model, the outer electrons are considered bound to a nuclear core by a restoring force proportional to the displacement from equilibrium ($-m_e \omega_0^2 x$). At equilibrium, the equation of motion for an electron is

$$m_e \frac{dx^2}{dt^2} + m_e \gamma \frac{dx}{dt} + m_e \omega_0^2 x = 0 \quad \text{II-14}$$

where ω_0 is the natural resonance of the system. If the electrons are acted upon by a harmonic electromagnetic wave of the form $E = E_0 e^{i\omega t}$, the system resembles a classical forced oscillator and Newton's second law yields

$$m_e \frac{d^2 x}{dt^2} + m_e \gamma \frac{dx}{dt} + m_e \omega_0^2 x = e E_0 e^{i\omega t} \quad \text{II-15}$$

Solutions to equation (II-15) are easily found by assuming a solution of the form of the forcing function. They yield

$$\bar{x} = \frac{e/m_e}{\omega_o^2 + \omega^2 + i\gamma\omega} E_o e^{i\omega t} \quad \text{II-16}$$

Substituting into (II-13), and canceling the field terms, yields

$$\tilde{n}^2 = 1 + \sum_{\ell} \frac{N_{\ell} e^2 / m_e \epsilon_o}{\omega_o^2 + \omega^2 + i\gamma\omega} \quad \text{II-17}$$

and we have the form of the complex index of refraction. Separating equation (II-17) into its real and imaginary components

$$\tilde{n} = n + iK \quad \text{II-18}$$

gives

$$n(\omega) = 1 + \frac{1}{2} \sum_{\ell} \frac{(N_{\ell} e^2 / m_e \epsilon_o)(\omega_{\ell}^2 - \omega^2)}{(\omega_{\ell}^2 - \omega^2) + \omega^2 \gamma_{\ell}^2} \quad \text{II-19}$$

$$K(\omega) = - \frac{1}{2} \sum_{\ell} \frac{(N_{\ell} e^2 / m_e \epsilon_o)(\omega \gamma_{\ell})}{(\omega_{\ell}^2 - \omega^2) + \omega^2 \gamma_{\ell}^2}$$

Kramers and Kronig first derived comparable equations from quantum mechanical considerations. Their equations are found in various texts, and the form published by Landau is shown for comparison.¹²

12. Landau, L. D., and Lifshitz, E. M., Electrodynamics of Continuous Media, translated from Russian by J. B. Sykes and J. J. Bell, p. 259, Addison-Wesley Publishing Company, 1960.

$$n(\omega) = 1 + \frac{1}{\pi} P \int_{-\infty}^{\infty} \frac{K(\omega') d\omega'}{\omega'^2 - \omega^2} \quad \text{II-20}$$

$$K(\omega) = -\frac{1}{\pi} P \int_{-\infty}^{\infty} \frac{n(\omega') - 1}{\omega'^2 - \omega^2} d\omega' \quad \text{II-21}$$

where P stands for the Cauchy principle value. Using the fact that $K(\omega)$ is an odd function

$$\tilde{n}(\omega) = 1 + \frac{2}{\pi} \int_0^{\infty} \frac{\omega' K(\omega') d\omega'}{\omega'^2 - \omega^2} \quad \text{II-22}$$

(II-18) can be rewritten in a more convenient form

$$n(\omega) = n(\omega) + iK(\omega) \quad \text{II-23}$$

where

$$n(\omega) = 1 + \delta(\omega) \quad \text{II-24}$$

or

$$n(E) = 1 + \delta(E) \quad \text{II-25}$$

and

$$\delta(E) = \frac{2}{\pi} \int_0^{\infty} \frac{E' K(E') dE'}{E'^2 - E^2} \quad \text{II-26}$$

where the equation is now considered in terms of the energy of the incident photons, $E = \hbar\omega$, and $\delta(E)$ is the variation of the index of refraction from unity.

Levinger¹³ demonstrates the absorption coefficient K is related to the total cross section of the individual atoms by

$$K(E) = \frac{Nc\hbar}{2E} \sigma(E) \quad \text{II-27}$$

or

$$2E \delta(E) = Nc\hbar\sigma(E). \quad \text{II-27a}$$

Substituting into (II-26)

$$\delta(E) = \frac{Nc\hbar}{\pi} \int_0^\infty \frac{\sigma(E') dE'}{E'^2 - E^2} \quad \text{II-28}$$

and we now have an expression for the variation from unity of the real part of the index of refraction in terms of the total cross section of the atom and the energy of the incident photon. Cooper¹⁴ states that the majority contribution to the index of refraction comes from photon energies significantly below 100 Rydberg (one Rydberg is 13.595 ev), and that in the region from zero to 100 Rydberg, the scattering cross section is negligible compared to the absorption cross section.

Up to the ionization threshold, the absorption cross section is composed of a series of discrete transitions defined by the transition rules of quantum mechanics. Beyond the ionization threshold, the absorption cross section is a continuum to the limits of integration. For

13. Levinger, J. S., letter dated 4 April 1979 to James Etchechury.

14. Cooper, J. W., "Photoionization from Outer Atomic Subshell. A Model Study," Physical Review, 128:681, 15 October 1962.

a discrete transition, the total absorption cross section is related to the oscillator strength for the line by

$$\int_{\text{line}} \sigma(E) dE = \frac{2\pi^2 e^2 \hbar}{mc} f_{nm} \quad \text{II-29}$$

The oscillator density for a line is related to the cross section by

$$\frac{df_{nm}}{dE} = \frac{mc}{2\pi^2 e^2 \hbar} \sigma(E) \quad \text{II-30}$$

which now defines the constant $R = \frac{mc}{2\pi^2 e^2 \hbar}$, and we can rewrite (II-28)

$$\delta(E) = C \left[\sum \frac{f_{nm}}{E_{nm}^2 - E^2} + \text{RP} \int_{\frac{1}{2}\hbar}^{\infty} \frac{\sigma(E') dE'}{E'^2 - E^2} \right] \quad \text{II-31}$$

where

$$C = \frac{N e \hbar}{\pi R}$$

E_{nm} is the discrete transition energy

E' is the variable of integration

and energy units are Rydbergs.

This formulation was used by Migneron¹⁵ to calculate $\delta(E)$ for Helium and by Liggett¹⁶ to calculate $\delta(E)$ for

15. Migneron, R. and J. S. Levinger, "Index of Refraction and Sum Rules for Helium," Physical Review, 13:A646-48, 2 August 1964.

16. Liggett, G. and J. S. Levinger, "Calculation of the Index of Refraction of Neon and Argon," Journal of the Optical Society of America, 58:1:109-113, January 1968.

Neon and Argon. Their theoretical results agree well with existing experiments, indicating good accuracy for this technique.

III. REVIEW OF THE OSCILLATOR STRENGTH

In order to evaluate the formula developed for the index of refraction, the oscillator strengths in absorption for the respective transition arrays are necessary. Condon and Shortley define a transition array as the totality of lines resulting from transitions between configurations (e.g., $1s^2 2s^2 2p^6$ to $1s^2 2s^2 2p^5 3s$). Bethe and Salpeter¹⁷ give the oscillator strength in a central field model for a single electron transition between configurations n and m , defined by quantum numbers $n\ell$ and $n'\ell'$.

$$\bar{f}_{nm} = \frac{1}{3} \frac{\ell_{\max}}{2\ell+1} (E_n - E_m) R_{nm}^2 \quad \text{III-1}$$

For $\ell' = \ell - 1$, $\ell_{\max} = \ell$, and for $\ell' = \ell + 1$, $\ell_{\max} = \ell + 1$, E_n and E_m are the energy eigenvalues of the states n and m . R_{nm} is the radial matrix element

$$R_{nm} = \int_0^\infty P_n(r) r P_m(r) dr \quad \text{III-2}$$

The single electron oscillator must be multiplied by the number of electrons in the outermost shell to determine the absolute oscillator strength.

Gruzdev¹⁸ has calculated the radial transition integrals for neon using a standard program which calculates the

17. Cited in Cooper, J. W., "Photoionization from Outer Atomic Subshells. A Model Study," Physical Review, 128:681, October 1962.

18. Gruzdev, P. F., and A. V. Loginov, "Neon, Radiative Lifetimes for the Levels of $2p^5ms$, $2p^5np$, $2p^5nd$ ($m = 3-6$, $n = 3-5$) and $2p^54f$ Configurations," Optics and Spectroscopy, 35:1-3, July, 1973.

Hartree-Fock radial wave equation for the configurations considered. These are reproduced in Table 2.

TABLE 2: Transition Integrals $\int P_n(r)rP_m(r)dr$ for Neon Atoms

Transition	HF	Transition	HF
3s-2p	0.43	3d-2p	0.11
3s-3p	4.76	3d-3p	6.3
3s-4p	0.35	3d-4p	9.22
3s-5p	0.13	3d-5p	0.11
4s-2p	0.17	4d-2p	0.081
4s-3p	4.25	4d-3p	1.6
4s-4p	10.91	4d-4p	11.4
4s-5p	1.07	4d-5p	19.2
5s-2p	0.10	5d-2p	0.06
5s-3p	0.98	5d-3p	0.82
5s-4p	10.3	5d-4p	3.22
5s-5p	19.34	5d-5p	17.68
6s-2p	0.069	4f-3d	10.2
6s-3p	0.51	4f-4d	15.9
6s-4p	12.06	4f-5d	1.74
6s-5p	18.2		

For equation III-1, an average level found by summing over the levels of the configuration given in Moore will be used in place of the energy eigenvalues used by Cooper, i.e.,

$$\bar{E} = \frac{\sum g_i E_i}{\sum g_i} \quad \text{III-3}$$

where i indicates the various energy levels of the configuration and g_i reflects the degeneracy or quantum statistical weight of the level.

While the energy eigenvalues could be found by evaluating the radial Schroedinger equation, Ligget's discussion of the calculation of the index of refraction cites difficulty in calculating energy eigenvalues. Use of published information for E_i was considered to be more accurate and, in addition, expedited the calculations.

IV. THE ABSORPTION CROSS SECTION

Extensive research data are available for Neon ($1s^2 2s^2 2p^6$). Since the demonstration of the Helium-Neon laser, a vast accumulation of theoretical and experimental work has occurred. It is safe to say that the important characteristics of the atom in its ground state are well known to researchers in this area. Not so well known are the characteristics of the metastable ($3s$) configuration; as a consequence, the accuracy of the available data for the photoionization cross section is not known.

Ederer and Tomboulia¹⁹ measured the total cross section of ground state neon from the ionization limit, 1.58 Rydberg. Their results are tabulated in the reference and plotted in Figs. 2 and 3. In his experiment, Ederer measured the transmission of ultraviolet light with the gas present and with vacuum. The cross section is given by

$$\sigma = \frac{1}{NL} \ln \left(\frac{I_0}{I} \right) \quad \text{IV-1}$$

where N is the density of atoms and L is the path length. To get monochromatic radiation, he used a normal incidence spectrograph. To measure the intensity of the current, both a photographic plate and a Geiger-Muller counter were used.

19. Ederer, D. L., and Tomboulia, D. H., "Photoionization Cross Section of Neon in 80-600A Region," Physical Review, 133:6A:1528, 16 March 1964.

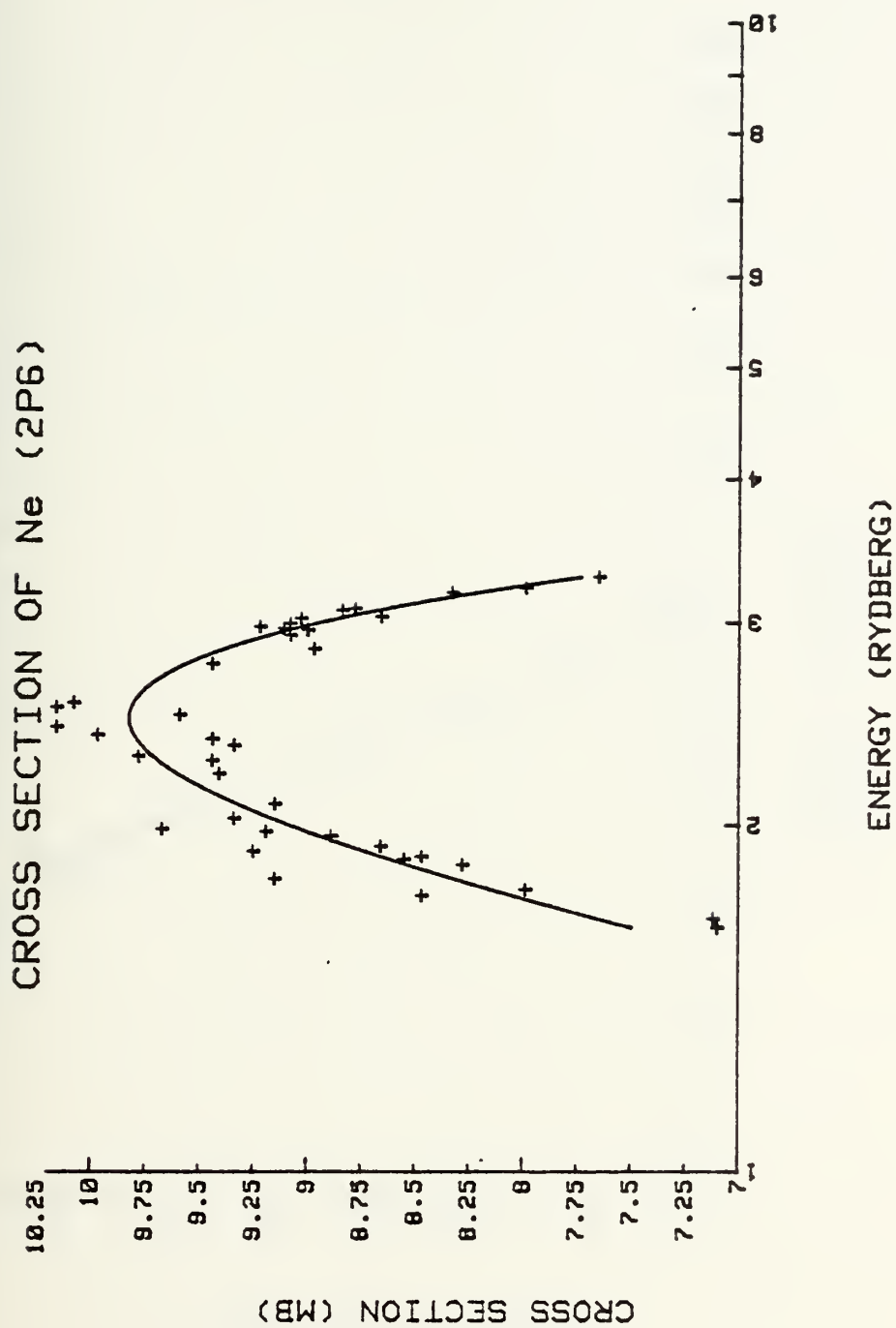


Figure 2. Photionization Cross Section of Neon ($2p^6$) in the Region 1.58 to 3.3 Rydberg.

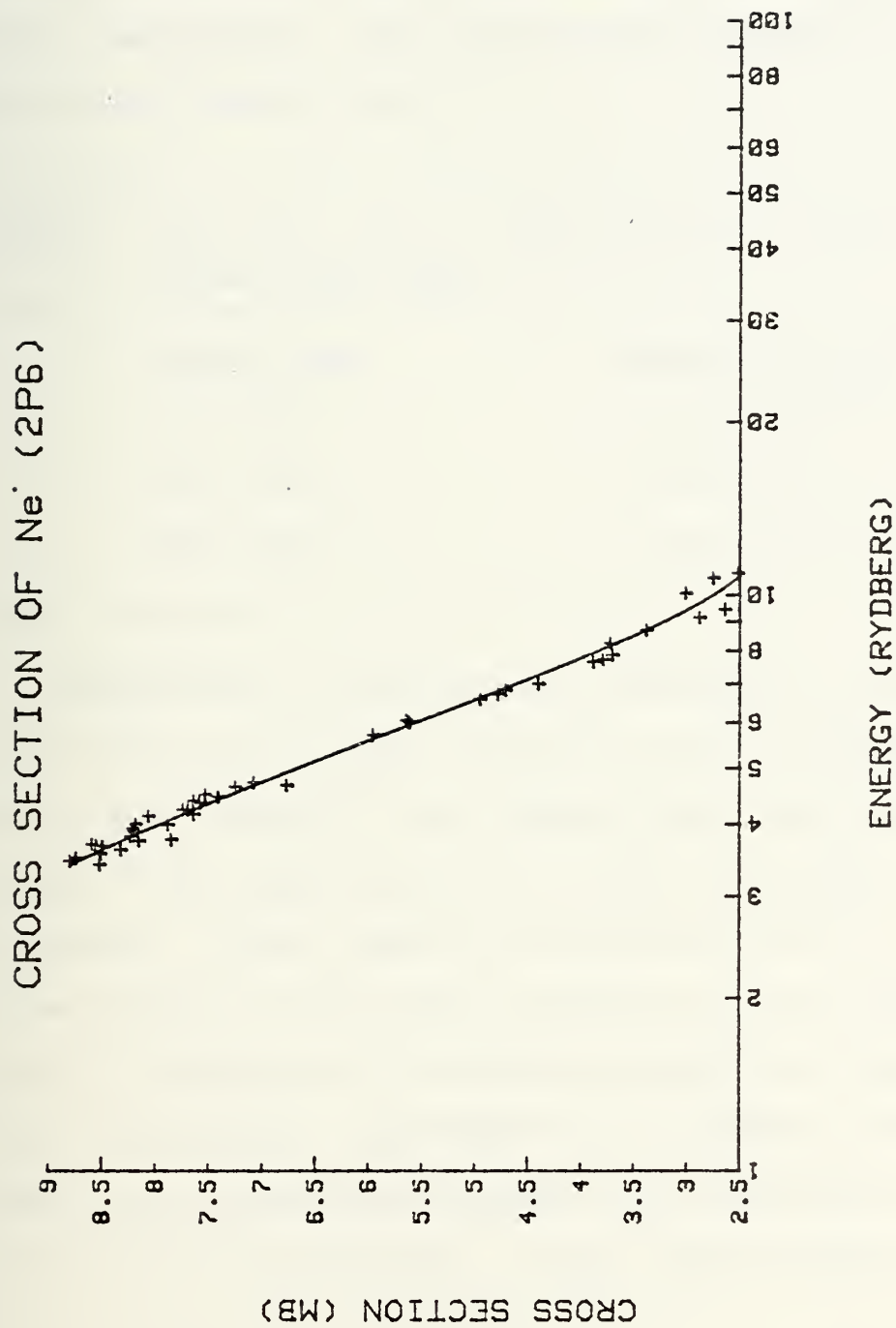


Figure 3. Photoionization Cross Section of Neon ($2p^6$) in the Region 3.3 to 11 Rydberg.

For energies above 12 Rydberg, Piech and Levinger²⁰ have fitted the cross section into a series of power laws. The power laws are fit to experimental data developed by other researchers. The laws and their respective limits are listed below: in Table 3:

TABLE 3: Empirical Fit for Photoionization Cross Sections Using Power Laws.

<u>Energy (Ry)</u>	<u>Cross Section (Mb)</u>
13.0-63.7	$1.12 \times 10^3 E^{-2.59}$
63.7-227.8	$3.24 \times 10^4 E^{-2.72}$
227.8-911.3	$1.10 \times 10^5 E^{-2.89}$

Theoretical and experimental knowledge of the photoionization of metastable rare-gas atoms is rather scarce. McCann and Flannery²¹ have employed the single particle central field approximation to examine the photoionization of Ne*(3s). Their results are plotted in Fig. 4. The cross section of the outer s electrons of the metastable gas as a function of the ejection energy has been found to yield considerable improvement over standard calculations based on an interaction obtained from iteration of the ground state configuration. These calculations demonstrate

20. Piech, K. R., and Levinger, J. S., "Sum Rules for Neon Photoeffect," Physical Review, 135:A332-6, March 1964.

21. McCann, K. J., and Flannery, M. R., "Photoionization of Metastable Rare-Gas Atoms," Applied Physics Letters, 31:9:601, 1 November 1977.

that the cross section is much smaller than that of Neon I and present an optical window in the 2000-3000 Å region. Although not in the immediate region of consideration (3510-3530 Å), the window is close enough to have considerable effect. Further inner shell ionization occurs only when relatively short wavelengths (@ 600 Å) are reached.

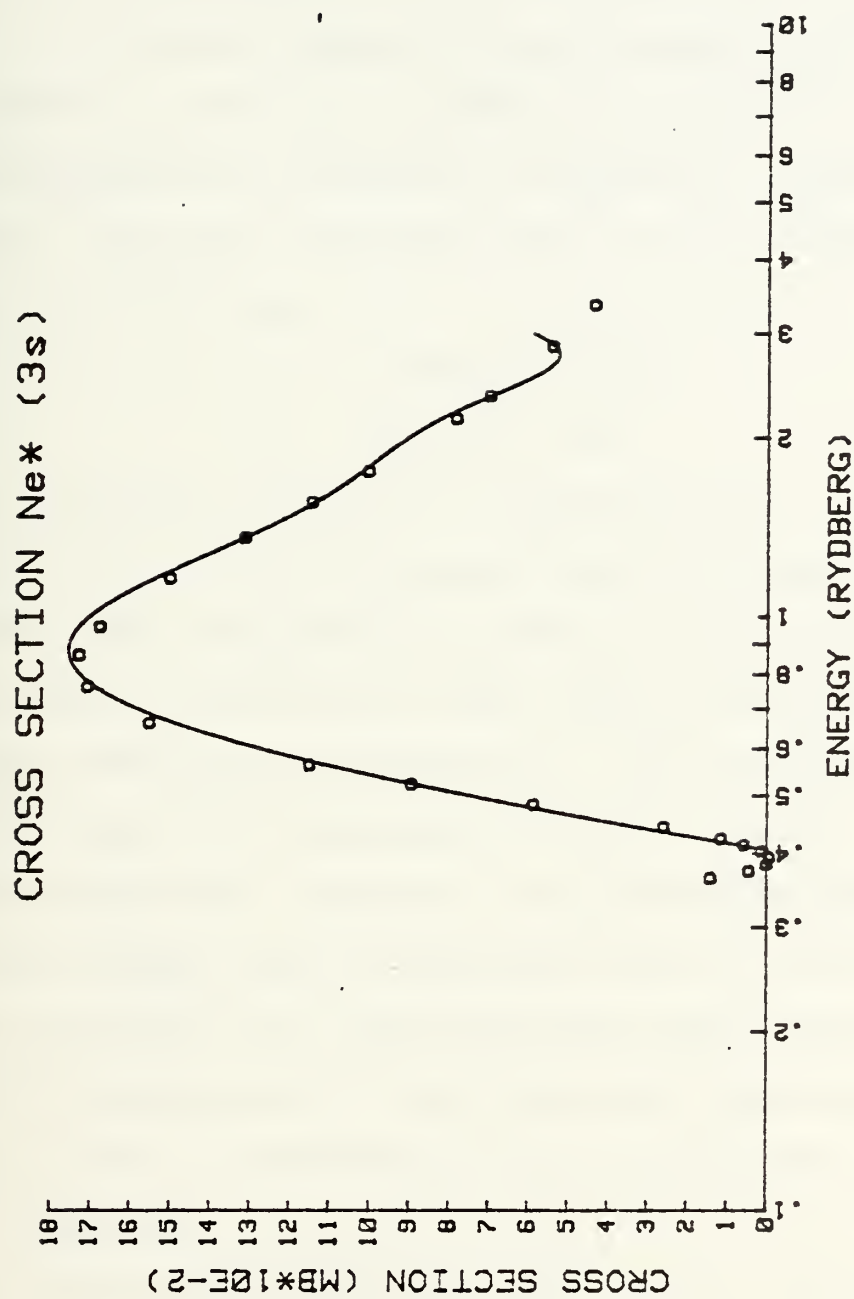


Figure 4. Photoionization Cross Section of Metastable Neon ($3s$)

V. CALCULATIONS OF THE INDEX OF REFRACTION OF NEON ($2p^6$)

Equation (II-31) was used to evaluate the index of refraction in the region of interest (3510-3530 Å, or .258 Ry), at standard temperature and pressure. If the cross section is measured in Megabarns ($1 \text{ Mb} = 10^{-18} \text{ cm}^2$) and the energies are considered in Rydbergs (1 Rydberg = 13.595 eV), then the respective value of the constants in equation (II-31) are:

$$C = 1.00009 \times 10^{-4} \text{ Ry}^2$$

$$R = .12895 \text{ Ry}^{-1} \text{ Mb}^{-1}$$

The oscillator strengths for the $2p \rightarrow (3s, 4s, 5s, 3d)$ transitions were calculated using Gruzdev's transition integrals. For the region of interest, the contribution to the index of refraction by inner shell ionization and any double excitation is negligible. The calculations agree well with the calculations of Cooper, except for the $2p \rightarrow 3d$ transition. However, this discrepancy between Cooper and Gruzdev does not adversely affect the results of the calculation due to the relatively small influence the $2p \rightarrow 3d$ transition has on the oscillator sum term of equation (II-31). The results of the calculations are given in Table 4.

The discrete cross sections above the 5s or 3d level become merged and insignificant relative to the numerical values of the lower transitions. This is clearly demonstrated in the calculations of Table 4 and in Figure 5.

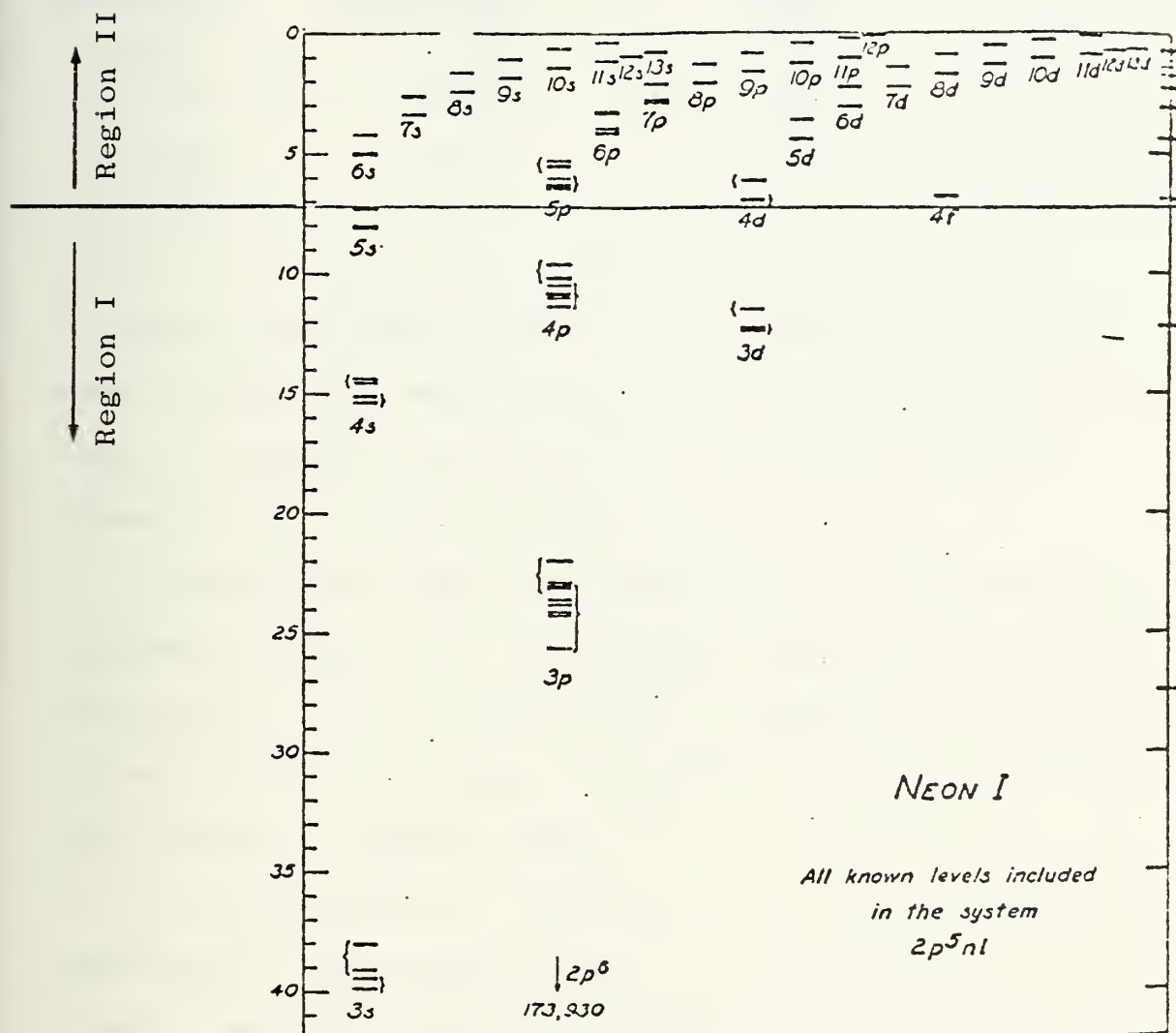


Figure 5. Energy Levels of Neon I and the Region of Discrete Oscillators Arrays (Region I) and Region of Extension of the Continuum Integral (Region II). (Scale in thousands of cm^{-1} .) (From Condon and Shortley, p. 302.)

Table 4. Transition Array Oscillator Strengths
for Ground State Neon ($2p^6$)

<u>Transition</u>	<u>Etchechury</u>	<u>Cooper</u>	<u>Process</u>
2p→3s	0.1632	0.1632	Absorption
4s	0.0279	0.0264	Absorption
5s	0.0102	0.0090	Absorption
3d	0.0239	0.0372	Absorption

To account for transitions to 5s and above, the continuum cross section data were extrapolated into this region; the limit of integration was adjusted to 1.51 Ry, which is determined by energy of the 5s level.

Adjusting the limit of integration in this manner is considered valid, since the discrete oscillator strength distribution can be considered as an extension of the continuum oscillator strength distribution. Cooper discusses this concept in greater detail.²³

In the continuum, a polynomial was fitted to Ederer's experimental cross section data in the region 1.58 to 3.3 Ry and a separate polynomial function from 3.3 to 13.0 Ry. This resulted in a set of polynomial functions that, when separated into individual components, resembled the form of the power laws developed by Piech for the region above 13.0 Ry.

23. Cooper, J. W., *ibid.*

The integral could be represented as a set of separate terms:

$$\int_{th}^{\infty} \frac{\sigma(E)dE'}{E'^2 - E^2} = \int_{1.51}^{3.3} + \int_{3.3}^{13.0} + \int_{13.0}^{63.7} + \int_{63.7}^{227.8} + \int_{227.8}^{911.8}$$

where the integral has been terminated at the upper limit of 911.8 Ry.

From Figs. 1 and 2 and Table 4, it is apparent that the major contribution to the index of refraction is made by the region near the ionization threshold. In the case of Neon, the contribution to the index from the region 1.51 Ry to 3.3 Ry, characterized by the peak in the cross section curve, is seventy-three percent of the continuum term. The region 3.3 Ry to 13.0 Ry contributes twenty-seven percent and the contribution from the region above this is so insignificant as to not be considered in these calculations. This does not result in any significant error and demonstrates that the majority of the photoionization to the index of refraction originates in the region near the ionization threshold. The small contribution at high energy is illustrated by the exceedingly small cross section that can be presumed by extrapolation of Fig. 3 to high energy. Comparison of results in Table 5 indicates good agreement for the Etchechury model, the more exhaustive calculations of Liggett, and the definitive experimental work of Cuthbertson. The results demonstrate that the simplification of the problem results in small error and the accuracy of the

Etchechury model is considered sufficient for application to the electronic species Ne*.

Table 5: Calculation of $\delta(E) = n-1$

<u>Author</u>	<u>Source</u>	<u>$(n-1) \times 10^4$</u>	<u>E</u>	<u>λ</u>
Etchechury	Theoretical	0.6705	0.258 Ry	3520 Å
Liggett	Theoretical	0.6778	0.25 Ry	3630 Å
	Theoretical	0.6825	0.30 Ry	3020 Å
Cuthbertson	Experimental	0.6788	0.25 Ry	3664 Å
	Experimental	0.6812	0.27 Ry	3342 Å

VI. CALCULATION OF THE INDEX OF REFRACTION OF NEON* (3s)

Equation (II-31) was used to evaluate the index of refraction of metastable Ne*(3s) at .258 Ry (3520 Å) and typical XeF cavity conditions. The conditions were standard temperature and pressure and an electron temperature of 13500°K due to pumping and kinetic action in the cavity. Using Boltzmann statistics with the assumed electron temperature of 13500°K, the ratio $N(\text{Ne}^*)/N(\text{NeI})$ is 1×10^{-6} . The respective values of the constants in equation (II-31) are:

$$C = 1.00009 \times 10^{-10} \text{ Ry}^2$$

$$R = 0.12895 \text{ Ry}^{-1} \text{ Mb}^{-1}$$

Drawing on the previous section, the Etchechury model was used to evaluate the index of refraction of Ne*(3s) in the region of interest at standard temperature and pressure. The oscillator strengths were calculated from Gruzdev's integrals for the 3s→(2p, 3p, 4p, 5p) transitions, as listed in Table 6. McCann and Flannery²⁴ indicated that inner shell ionization and double excitation is negligible.

The oscillator strengths calculated by Cooper's method were verified by means of the polarizability equation and

24. McCann, K. J. and M. R. Flannery, "Photoionization of Metastable Rare-Gas Atoms," Applied Physics Letters, 31:9:599, November 1977.

the calculations of Cohen and Schnieder.²⁵ They use:

$$\bar{\alpha} = \frac{e^2 \hbar^2}{m_e} \sum_m \frac{f_{nm}}{(E_n - E_m)^2} \quad \text{VI-1}$$

with the results listed in Table 7.

Table 6. Transition Array Oscillator Strengths for Ne*(3s)

Transition	f	E _{nm} (Ry)	Process
3s→2p	-0.0482	1.230	Emission
3p	1.080	0.146	Absorption
4p	0.0106	0.259	Absorption
5p	0.00129	0.0302	Absorption

By comparison, summing over the oscillator strength of Table 6 and adjusting for one electron value gives:

$$\alpha = 32.492 \approx 32.5 (\times 10^{-24} \text{ cm}^3).$$

This agrees well with the calculations of Table 7 and demonstrates the accuracy attainable with the Etchechury model.

Table 7. Polarizability of Ne*

State (Ne*)	($\times 10^{-24} \text{ cm}^3$)
³ P ₂	28.2
³ P ₁	29.2
³ P ₀	29.2
¹ P ₁	33.4

25. Cohen, S., and B. Schneider, "Ground and Excited States of Ne₂ and Ne₂⁺," Journal of Chemical Physics, 61:8, p. 3238, 15 October 1974.

The contribution to the index of refraction of the discrete transition is $\delta'(E) = \sum \frac{f_{nm}}{E_{nm}^2 - E^2}$. The summation term indicates that any term having a transition energy near the laser cavity resonance radiation frequency (.258 Ry, 3520 Å) will have a significant contribution to the index of refraction. From Table 6, it is apparent that the energy of the 3s→4p transition ($\bar{E}_{nm} = .259$ Ry) is near the cavity resonance energy, and requires consideration of the individual lines that comprise the transition array. This implies that the sum over the discrete transition terms in equation (II-31) is as shown in Table 8.

Table 8. Contribution of Discrete Transitions to n-1

<u>Transition</u>	<u>Terms in Series</u>
3s→2p	Use array term (negative for emission)
3p	Use array term
4p	Use summation over 30 lines
5p	Use array term
....	Above 5p included in continuum integral

In the transition array, there are forty possible transitions between the four 3s levels ($1s_2, 1s_3, 1s_4, 1s_5$, in the Paschen notation) and the ten 4p levels ($3p_i$, where $i=1,10$). Because of selection rules on J, ten of the lines are eliminated, leaving thirty lines for consideration. The relative line strengths for the transitions can be determined from Table 4 of Semenov and Strugach.²⁶ The relative line strengths are

26. Semenov, R. I., and B. A. Strugach, "Determination of Coupling Coefficients for the np^5n' 's and np^5n' 'p Configurations from Experimental Data," Optics and Spectroscopy, 24:, p. 260, April 1968.

indicated as the upper number and the corresponding oscillator strength is the lower number in Table 7. The levels of the 4p configuration are arrayed in order of decreasing energy across the top. The 3p₅ level is at lower energy than the 3p₃.

Table 9. Relative line strengths (upper number) and oscillator strengths (lower number) for 3s→4p transition.

K	1	2	3	4	5	6	7	8	9	10	
	3p ₁₀	3p ₉	3p ₈	3p ₇	3p ₆	3p ₃	3p ₅	3p ₂	3p ₄	3p ₁	J
2s ₂	.056	0	0	0.139	.833	.111	.667	.333	.833	.333	4
	.0015	J		0.0036	.0216	.0029	.0173	.0066	.0216	.0066	
2s ₃	.056	0	0	.278	0	0	.333	.333	0	0	3
	.0044	J	J	.0216	J	J	.0259	.0259	J	J	
2s ₄	.250	0	1.375	.625	.083	.222	0	.125	.208	.111	2
	.0065	J	.0356	.0162	.0021	.0057		.0032	.0054	.0029	
2s ₅	.694	2.333	.292	.097	.750	0	0	.208	.625	0	1
	.0108	.0361	.0046	.0016	.0116	J		.0032	.0097	J	

Note: Paschen notation is used to identify levels.

The indices K,J refer to the transitions listed in Fig. 7.

In order to clarify the contribution of the 3s→4p transition to the index of refraction, we consider the summation term in equation (II-31) in terms of cavity wavelength:

$$\delta'(E) = C \sum \frac{f_{nm}}{E_{nm}^2 - E^2} = \frac{Ne^2}{2\pi mc} \sum \frac{\lambda_{nm}^2 \lambda^2}{\lambda^2 - \lambda_{nm}^2} f_{nm} \quad \text{VI-2}$$

Figure 6 is a plot of function VI-2, using values for f_{nm} from Table 9. Line width and damping are not considered in

these calculations. Without these considerations, the contributions to n approaches infinity at line resonance.

Examination of Figure 7 indicates anomalous dispersion at 351.2, 351.6, and 351.2. The $2s_4 \rightarrow 3p_8$ transition is the source at 351.6, the $2s_2 \rightarrow 3p_1$ transition at 352.1, and the $2s_5 \rightarrow 3p_{10}$ transition at 352.1.

As before, the discrete cross sections above 5p level become merged and indistinct, and the continuum cross section data is extrapolated into this region. A polynomial was fitted to the calculations of McCann and Flannery to generate a function for the integrand of equation II-28 of the form of the previous section. The data and the polynomial approximation used in the region near the peak cross section are indicated in Fig. 4. Ionization threshold for $Ne^*(3s)$ is 0.365 Ry and the lower limit of integration is extended to 0.360 Ry, determined by the energy of the 5p level. The form of the integral is:

$$\int_{th}^{\infty} \frac{\sigma(E')dE'}{E'^2 - E^2} \approx \int_{.360}^{.395} + \int_{.395}^{3.3}$$

The integration extends only to 3.3 Ry, due to the fact the results of McCann and Flannery terminate at that energy. The question arises as to the extent of error introduced by neglecting the integral from 3.3 Ry to infinity. Previous calculations demonstrate the order of magnitude of the error introduced by termination of the integral nearer the ionization level. Since data are not available for the cross section beyond 3.3 Ry level, an extrapolation of the relationship

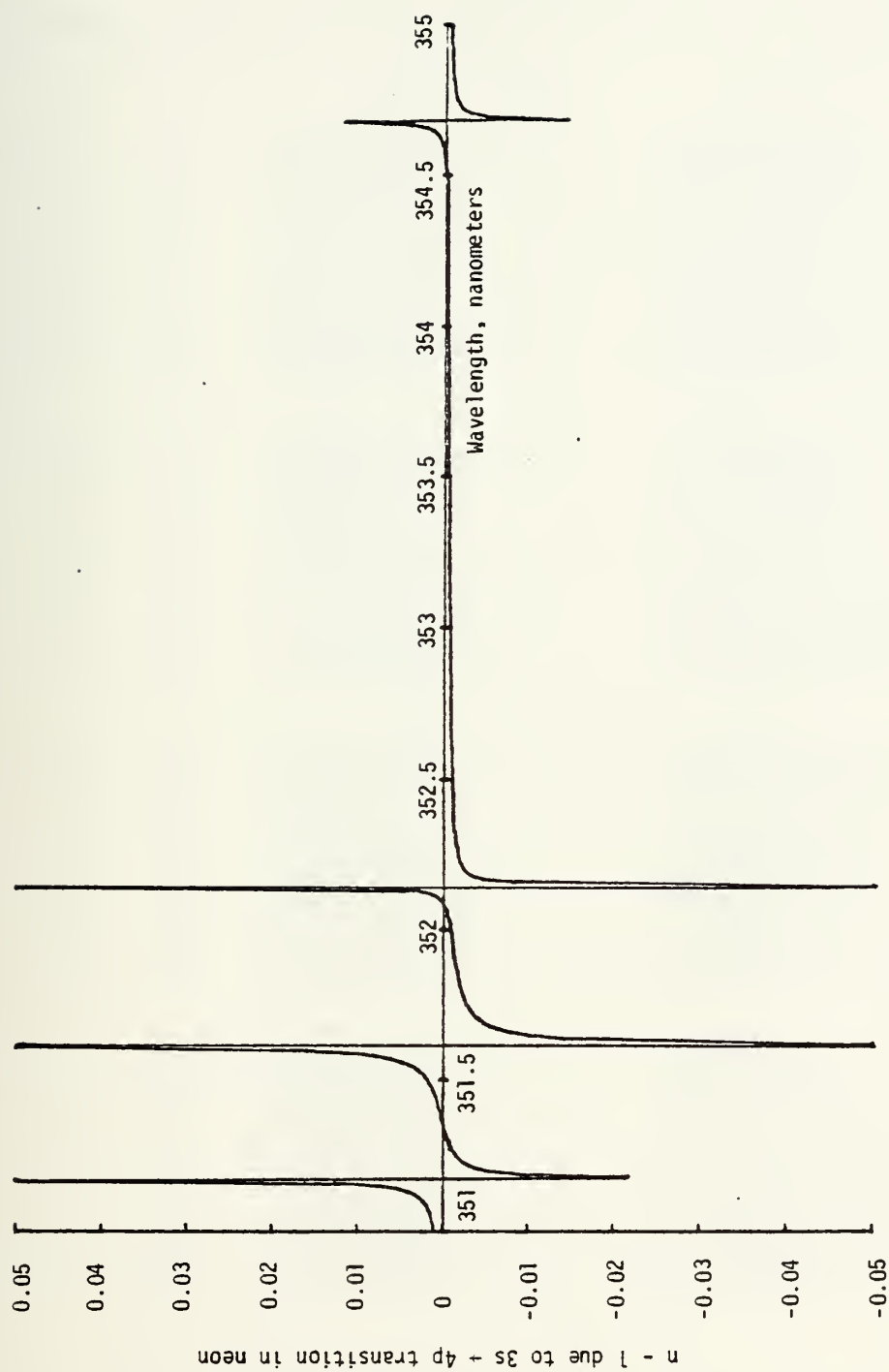


Figure 6. Contribution of 3s \rightarrow 4p Transition in Neon* to δ' as a Function of Wavelength.

THIS PROGRAM CALCULATES THE CONTRIBUTION OF 3S TO 4P TRANSITION IN NE+
 THE WAVELENGTH OF THE XEF LASER RADIATION IS 352 NANOMETER.

J	K	W(J,K)	G(J)	N(J,K)	SUM
1	1	3.511729E-05	5	-1.6999042E-03	-1.6999042E-03
1	2	3.473549E-05	5	-9.9867240E-04	-2.6985782E-03
1	3	3.465364E-05	5	-1.0608307E-04	-2.8046089E-03
1	4	3.451728E-05	5	-2.8131199E-05	-2.8327017E-03
1	5	3.448752E-05	5	-2.0739388E-04	-3.0401811E-03
1	6	3.406111E-05	5	0.0000000E+00	-3.0401811E-03
1	7	3.376667E-05	5	0.0000000E+00	-3.0401811E-03
1	8	3.370862E-05	5	-2.6600256E-05	-3.0667846E-03
1	9	3.370749E-05	5	-7.9827924E-05	-3.1466127E-03
1	10	3.306441E-05	5	0.0000000E+00	-3.1466127E-03
2	1	3.563919E-05	3	1.1786284E-04	-3.0287400E-03
2	2	3.524602E-05	3	0.0000000E+00	-3.0287400E-03
2	3	3.516174E-05	3	-7.2954210E-03	-1.0324171E-02
2	4	3.502136E-05	3	-7.0812808E-04	-1.1032265E-02
2	5	3.499073E-05	3	-7.9934359E-05	-1.1112233E-02
2	6	3.455186E-05	3	-6.7795567E-05	-1.1180029E-02
2	7	3.424892E-05	3	0.0000000E+00	-1.1180029E-02
2	8	3.418920E-05	3	-2.4056824E-05	-1.1204066E-02
2	9	3.418803E-05	3	-3.9907764E-05	-1.1243907E-02
2	10	3.352667E-05	3	-1.2546584E-05	-1.1256540E-02
3	1	3.610239E-05	1	1.3085913E-05	-1.1243454E-02
3	2	3.569899E-05	1	0.0000000E+00	-1.1243454E-02
3	3	3.561254E-05	1	0.0000000E+00	-1.1243454E-02
3	4	3.546854E-05	1	2.1301336E-04	-1.1030441E-02
3	5	3.543712E-05	1	0.0000000E+00	-1.1030441E-02
3	6	3.498705E-05	1	0.0000000E+00	-1.1030441E-02
3	7	3.467647E-05	1	-1.2641887E-04	-1.1156398E-02
3	8	3.461525E-05	1	-1.1288197E-04	-1.1269740E-02
3	9	3.461405E-05	1	0.0000000E+00	-1.1269740E-02
3	10	3.393627E-05	1	0.0000000E+00	-1.1269740E-02
4	1	3.755304E-05	3	5.3489779E-06	-1.1264391E-02
4	2	3.711677E-05	3	0.0000000E+00	-1.1264391E-02
4	3	3.702332E-05	3	0.0000000E+00	-1.1264391E-02
4	4	3.686772E-05	3	1.8075789E-05	-1.1246315E-02
4	5	3.683377E-05	3	1.1113251E-04	-1.1135101E-02
4	6	3.634778E-05	3	2.0551615E-05	-1.1114541E-02
4	7	3.601268E-05	3	1.7237523E-04	-1.0942179E-02
4	8	3.594666E-05	3	9.3551651E-05	-1.0848601E-02
4	9	3.594536E-05	3	2.3488048E-04	-1.0613730E-02
4	10	3.521499E-05	3	4.5192963E-03	-6.0944370E-03

Figure 7. Sample Computer Output for the Calculation of the Contribution to the Index of Refraction of the 3s→4p Transition.

THIS PROGRAM CALCULATES THE CONTRIBUTION OF 3S TO 4P TRANSITION IN NE*

THE WAVELENGTH OF THE XEF LASER RADIATION IS 351 NANOMETER.

J	K	W(J,K)	G(J)	N(J,K)	SUM
1	1	3.511729E-05	5	9.079849E-04	9.0798491E-04
1	2	3.473549E-05	5	-1.416327E-04	7.6635222E-04
1	3	3.465364E-05	5	-1.468576E-05	7.5166647E-04
1	4	3.451728E-05	5	-3.889636E-06	7.4777683E-04
1	5	3.448752E-05	5	-2.679485E-05	7.2098198E-04
1	6	3.406111E-05	5	0.000000E+00	7.2098198E-04
1	7	3.376667E-05	5	0.000000E+00	7.2098198E-04
1	8	3.370862E-05	5	-3.143693E-06	7.1783828E-04
1	9	3.370749E-05	5	-9.521060E-06	7.0831722E-04
1	10	3.306441E-05	5	0.000000E+00	7.0831722E-04
2	1	3.563919E-05	3	1.075017E-05	7.1906739E-04
2	2	3.524602E-05	3	0.000000E+00	7.1906739E-04
2	3	3.516174E-05	3	5.038766E-04	1.2239440E-03
2	4	3.502136E-05	3	-1.789580E-04	1.0439860E-03
2	5	3.499073E-05	3	-1.667250E-05	1.0273135E-03
2	6	3.455186E-05	3	-8.852035E-06	1.0184614E-03
2	7	3.424892E-05	3	0.000000E+00	1.0184614E-03
2	8	3.418920E-05	3	-2.943663E-06	1.0155178E-03
2	9	3.418803E-05	3	-4.960808E-06	1.0105570E-03
2	10	3.352667E-05	3	-1.499386E-05	1.0090576E-03
3	1	3.610239E-05	1	1.330212E-06	1.0103878E-03
3	2	3.569899E-05	1	0.000000E+00	1.0103878E-03
3	3	3.561254E-05	1	0.000000E+00	1.0103878E-03
3	4	3.546854E-05	1	1.729702E-05	1.0276848E-03
3	5	3.543712E-05	1	0.000000E+00	1.0276848E-03
3	6	3.498705E-05	1	0.000000E+00	1.0276848E-03
3	7	3.467647E-05	1	-1.744620E-05	1.0102386E-03
3	8	3.461525E-05	1	-1.520255E-05	9.9503605E-04
3	9	3.461405E-05	1	0.000000E+00	9.9503605E-04
3	10	3.393627E-05	1	0.000000E+00	9.9503605E-04
4	1	3.755304E-05	3	5.894808E-07	9.9562553E-04
4	2	3.711677E-05	3	0.000000E+00	9.9562553E-04
4	3	3.702332E-05	3	0.000000E+00	9.9562553E-04
4	4	3.686772E-05	3	1.910255E-06	9.9753579E-04
4	5	3.683377E-05	3	1.166996E-05	1.0092057E-03
4	6	3.634778E-05	3	2.134400E-06	1.0113401E-03
4	7	3.601268E-05	3	1.716881E-05	1.0285090E-03
4	8	3.594666E-05	3	9.175135E-06	1.0376841E-03
4	9	3.594536E-05	3	2.307851E-05	1.0607626E-03
4	10	3.521499E-05	3	6.550919E-05	1.1262718E-03

Figure 8. Sample Computer Output for the Calculation of the Contribution to the Index of Refraction of the 3s+4p Transition.

found in the calculations for unexcited neon was used. This implies that the cross section curves of Neon I and Ne*(3s) have similar shapes characterized by a peak near the ionization threshold and a sloping off to an asymptotic minimum value. Intuitively, this approach appears correct if we compare the shape of the curves near the ionization threshold. A more rigorous discussion was not attempted.

From Section V, the contribution to the continuum integral of the region near the peak is .73 of the total contribution. Modifying equation (II-31) by including the weighting factor

$$\delta(E) = C \left[\sum \frac{f_{nm}}{E_{nm}^2 - E^2} + BR \int_{.360}^{3.3} \frac{\sigma(E') dE'}{E'^2 - E^2} \right] \quad \text{VI-3}$$

where $B = (1/.73) = 1.37$. Calculation of the variation of the index of refraction from unity, using equation (VI-3) yields

$$\delta(E) = -7.79 \times 10^{-10}.$$

VII. COMPARISON OF RESULTS OF CALCULATION

The phase shifts across the cavity aperture per unit length of cavity may be obtained using the relation

$$\frac{\Delta\phi}{L} = - \frac{\delta(E)}{\lambda} \quad \text{VII-1}$$

where L and λ are expressed in consistent units. A lag in phase relative to vacuum is treated as a negative phase angle. Evaluating equation (VII-1) at 3520 Å and introducing the value of $\delta(E)$ calculated in the previous section yields:

$$\frac{\Delta\phi}{L} = 2.213 \times 10^{-3} \text{ m}^{-1}$$

Accuracy of the calculation is limited by the available cross section data beyond the ionization threshold. Improvement in the calculation would result from extension of the cross section calculations used in Section VI to an asymptotic minimum value, as has been done in the case of Neon I.

Hunter²⁷, in a separate approach to the problem, calculates the phase shift due to Ne* to be $2 \times 10^{-5} \text{ cm}^{-1}$.

The model developed in this paper demonstrates good agreement with independent research and is applicable to any atomic species present in the XeF cavity. The accuracy is dependent on (a) the availability of cross section data beyond the ionization threshold of the species under consideration, and (b) estimates of the species population in the cavity. Current

27. Hunter, R. O., "Draft on Transient Index of Refraction in HgCl and XeF Lasers," unpublished report, Western Research Corporation, Los Angeles, CA, p. 17, April 1978.

research into development of a populations model is being conducted by LT Lonnie Cole as a continuation of this research.

BIBLIOGRAPHY
(Books)

- Bates, D. R., (ed.), Atomic and Molecular Processes, pp. 47-54, Academic Press, 1962.
- Condon, E. U., and Shortley, G. H., The Theory of Atomic Spectra, Cambridge, 1963 (reprint of 1932 ed.).
- Hartree, D. R., The Calculation of Atomic Structure, Wiley, 1957.
- Jackson, J. D., Classical Electrodynamics, Wiley, 1962.
- Landau, L. D., and Lifshitz, E. M., Electrodynamics of Continuous Media, translated from Russian by J. B. Sykes and J. J. Bell, Addison-Wesley, 1960.
- Mitchell, A. C. G., and Zemansky, M. W., Resonance Radiation and Excited Atoms, Cambridge, 1934.
- Pauling, L., and Wilson, E. B., Introduction to Quantum Mechanics, McGraw-Hill, 1935.

BIBLIOGRAPHY
(Articles and Reports)

- Afanaseva, N. V., and P. F. Gruzdev, "Lifetimes of ns and np Levels of a Neon Atom," Optics and Spectroscopy, 38:211, February, 1975.
- Bakos, J., and J. Szigeti, "Average Lifetime of 2p Levels of Neon," Optics and Spectroscopy, 23:255-56, September, 1967.
- Boness, M. John W., and H. A. Hyman, "Investigation of Electron Impact Processes Relevant to Visible Lasers," Semi-Annual Report for Periods 1 March 1976 to 31 August 1976, Everett, Massachusetts: Avco Everett Research Laboratory, Inc., 53 pp.
- _____, "Investigation of Electron Impact Processes Relevant to Visible Lasers," Semi-Annual Report for Period I, March 1977 to 31 August 1977, Everett, Massachusetts: Avco Everett Research Laboratory, Inc., 53 pp.
- Carter, Steven L., and Hugh P. Kelly, "Double Photoionization of Neon and Argon," Physical Review A, 16:1525-1534, October 1977.
- Chashchina, G. I., and E. Ya. Shreider, "Determination of the Oscillator Strengths of the Resonance Lines of Krypton," Optics and Spectroscopy, 22:284-85, March 1967.
- _____, "Determination of Xenon and Krypton Refractive Indices in the Vacuum Region of the Spectrum," Optics and Spectroscopy, 27:79-80, July, 1969.
- Codling, K., R. P. Madden, and D. L. Ederer, "Neon Cross Section," Physical Review, 155:26, 1967.
- Cohen, S., and B. Schneider, "Ground and Excited States of Ne₂ and Ne₂⁺," Journal of Chemical Physics, 61:8, p. 3238, 15 October 1974.
- Cooper, John W., "Photoionization from Outer Atomic Subshells. A Model Study," Physical Review, 128:681-93, October 1962.
- Ederer, D. L., and Tombouljian, D. H., "Photoionization Cross Section of Neon in 80-600 Å Region," Physical Review, 133:6A:1525-1532, 16 March 1964.
- Galkin, V. D., and R. I. Semenov, "g-Factors of Neon 2s Levels," Optics and Spectroscopy, 29:544-45, November, 1970.
- Gold, Albert, and Robert S. Knox, "Excited State Wave Functions, Excitation Energies, and Oscillator Strengths for Ne(2p⁵3s)," Physical Review, 113:834-39, 1 February 1959.

- Gruzdev, P. F., "Oscillator Strengths of Resonance Lines in the Spectra of Ne I, Ar I, Kr I, Xe I Atoms and Na II and Rb II Ions," Optics and Spectroscopy, 22:170-7-, February, 1967.
- Gruzdev, P. F., and A. V. Loginov, "Neon, Radiative Lifetimes for the Levels of $2p^5ms$, $2p^5nd$ ($m = 3-6$, $n = 3-5$) and $2p^54f$ Configurations," Optics and Spectroscopy, 35:1-3, July, 1973.
- _____, "Neon Transition Probabilities, Part 2: $2p^54p-2p^5ns$ ($n = 3-6$) Transitions," Optics and Spectroscopy, 39:464-65, November, 1975.
- Gubin, M. A., A. I. Popov, and E. D. Protsenko, "Pressure Dependence on the Line Width of the $3s_2-3p_4$ Transition," Optics and Spectroscopy, 25:421-22, November, 1968.
- Hay, P. J., and T. H. Dunning, Jr., "The Electronic States of KrF," The Journal of Chemical Physics, 66:1306-16, 1 February 1977.
- Hunter, R. O., "Draft on Transient Index of Refraction in KeF and HgCl Lasers," (Unpublished), April 1978.
- Kotlikov, E., and M. Chaika, "Radiation Lifetime of the $3p_4$ State of Ne," Optics and Spectroscopy, 27:281-82, September, 1969.
- Krivchenkova, V. S., "Absolute Spontaneous Transition Probabilities in the Ne Atom," Optics and Spectroscopy, 25:536, December, 1968.
- Liggett, G. and J. S. Levinger, "Calculation of the Index of Refraction of Neon and Argon," Journal of the Optical Society of America, 58:109-13, January, 1968.
- McCann, K. J., and M. R. Flannery, "Photoionization of Metastable Rare-Gas Atoms," Applied Physics Letters, 31:9:599-601, November, 1977.
- McDaniel, E. W., et al., "Compilation of Data Relevant to Gas-Rare Gas and Rare Gas-Monohalide Excimer Lasers," Volume I, Technical Report H-78-1, Redstone Arsenal, Alabama: High Energy Laboratory, U. S. Army Missile Research and Development Command, 427 pp., December, 1977.
- _____, "Compilation of Data Relevant to Rare Gas-Rare Gas-Monohalide Excimer Lasers," Volume II, Technical Report H-78-1, Redstone Arsenal, Alabama: High Energy Laser Laboratory, U. S. Army Missile Research and Development Command, pp. 428-894, December, 1977.

- Moore, Charlotte E., "Atomic Energy Levels, Volume I, Hydrogen Through Vanadium," NBS Circular 367, U. S. Government Printing Office, Washington, D. C., 309 pp., 15 June 1949.
- Oshirovich A. L., and Ya, F. Verolainen, "Radiative Lifetimes and the Mechanism of Population and Depopulation of Neon Levels," Optics and Spectroscopy, 22:181-84, March, 1967.
- Rockwell International, "XeF Demonstrator Program," by R. Siegler, et al., pp. 191-92, 15 February 1979.
- Semenov, R. I., and B. A. Strugach, "Determination of Coupling Coefficients for the np^5n 's and $np^5n'p$ Configurations from Experimental Data," Optics and Spectroscopy, 24:258-62, April, 1968.
- Sewell, Kenneth G., "Inert-Core Hartree-Fock Approximation as Applied to Some Autoionizing States of Neon," Journal of the Optical Society of America, 55:739-40, June, 1965.
- Wadt, W. L., D. C. Cartwright, and J. S. Cohen, "Theoretical Absorption Spectra for Ne_2^+ , Ar_2^+ , Kr_2^+ , and Xe_2^+ in the Near Ultraviolet," Applied Physics Letters, 31:10:672-74, 15 November 1977.
- Wiese, W. L., et al., "Atomic Transition Probabilities, Volume I, Hydrogen Through Neon," NBS Reference Data Service, National Bureau of Standards, 157 pp., 04 May 1966.

INITIAL DISTRIBUTION LIST

	No. Copies
1. Defense Documentation Center Cameron Station Alexandria, Virginia 22314	2
2. Library, Code 0142 Naval Postgraduate School Monterey, California 93940	2
3. Chairman, Code 61 Department of Physics and Chemistry Naval Postgraduate School Monterey, California 93940	2
4. Office of Research Administration, Code 012A Naval Postgraduate School Monterey, CA 93940	1
5. Professor Allen E. Fuhs, Code 61Fu Department of Physics and Chemistry Naval Postgraduate School Monterey, California 93940	6
6. Major Rett Benedict DARPA 1400 Wilson Boulevard Arlington, Virginia 22209	2
7. Dr. Joseph Mangano DARPA 1400 Wilson Boulevard Arlington, Virginia 22209	2
8. Dr. William J. Condell Office of Naval Research Code 421 800 Quincy Boulevard Arlington, Virginia 22217	1
9. Dr. Robert Behringer Office of Naval Research Pasadena Branch Office 1030 East Green Street Pasadena, California 91101	1

Thesis
E7125
c.1

Etchechury

183837

A simple model for
calculating the in-
dex of refraction
of Neon I and Neon*
(3s) in the cavity
of a Xenon Flouride
laser.

Thesis
E7125
c.1

Etchechury

183837

A simple model for
calculating the in-
dex of refraction
of Neon I and Neon*
(3s) in the cavity
of a Xenon Flouride
laser.

DUDLEY KNOX LIBRARY



3 2768 00033010 4